

High efficiency Pb(II) removal using a green synthesized biochar/graphene-supported chlorapatite

B. Zeng^{a,b,*}, W.F. Liu^a

^aCollege of Mechanical Engineering, Hunan University of Arts and Science, Changde 415000, People's Republic of China

^bHunan Collaborative innovation Center for construction and development of Dongting Lake Ecological Economic Zone, Changde 415000, People's Republic of China

Carbonaceous nano-chlorapatites have attracted great attention for the remediation of heavy metal-contaminated environment. Herein, a novel biochar/graphene-supported chlorapatite (BC/G-ClAP) was successfully synthesized by a green method for the purpose of removing the Pb(II) from the water. The generated BC/G-ClAP was characterized by Scanning electron microscope (SEM) and transmission electron microscopy (TEM). It was found that biochar had the mesoporous structure with the layers of graphene on biochar surfaces and chlorapatites were distributed on the surface of biochar/graphene. BC/G-ClAP showed excellent remediation performance towards Pb(II) contaminated water, with the Pb(II) removing efficiency of 80.29%. The high remediation was due to the porous biochar/graphene with plenty of functional group have the strong adsorption for the Pb(II) ions and the chlorapatites showed the cation exchange with Pb(II) to form the stable $Pb_{10}(PO_4)_6Cl_2$. Therefore, this green synthesis method and the novel composites have a great potential for the application of remediation in the contaminated environment.

(Received February 17, 2022; Accepted April 20, 2022)

Keywords: Biochar, Graphene, Lead, Chlorapatite.

1. Introduction

Toxic heavy metal pollution, which is non-biodegradable and bio-accumulative, is the environmental issue of global concern. Particularly, lead (Pb) can result in anaemia and renal tubular damage^[1]. Thus, it is significant to seek an effective method to eliminate its contamination. Until now, some technologies have been used to remediate Pb(II) pollution, including ion exchange^[2], biological treatment^[3], reduction^[4], precipitation^[5], electro dialysis^[6], and adsorption^[7], et al.

Recently, Chlorapatite [$Ca_{10}(PO_4)_6Cl_2$] (ClAP) has drawn significant attention to for remediation of heavy metal polluted environment, in which they have strong affinities Pb(II) ions for their negatively charged phosphate groups and can also establish cation exchange reaction to form stable $Pb_{10}(PO_4)_6Cl_2$ with Pb(II) ions, thus resulting in reducing their toxicity^[8]. Hence, ClAP has a great potential in the heavy metals removing.

However, the ClAP particles usually exist in large sizes and thus limit their remediation effect^[9]. Therefore, developing biochar-based nanocomposites is a new direction with the following advantage. One is that biochar with the high specific area can serve as an ideal support for loading nanoparticles and decrease the aggregation of nanoparticles^[10]. The second is that biochar with porous structure have strong affinity to the metal ions^[11]. Thus, considerable research has been focused on synthesis of biochar-supported chlorapatite (BC-CLAP) nanocomposites.

On the other hand, graphene nanosheets (G) are composed of a basal plane with plenty of bearing oxygen functionalities^[12]. Thus, the combination of biochar and graphene is an effective sorption agent for various environmental contaminants^[13]. Furthermore, graphene-containing

* Corresponding author: 21467855@qq.com
<https://doi.org/10.15251/DJNB.2022.172.541>

biochar can possess a lot of improvement in physicochemical properties, including surface area, pore volume, surface functional groups, thermal stability, and electron transfer capability, leading to a greatly enhanced environmental remediation potential.

Taking into consideration all the aspects discussed above, our study reported the fabrication of a novel biochar/graphene-supported chlorapatite via hydrothermal and carbonization. The removing Pb(II) from the water solution was also explored and the potential mechanism was further elucidated. The results show that BC/G-CLAP had the large surface, porous structure with abundant CLAP nanoparticles, leading to the improved Pb(II) removing.

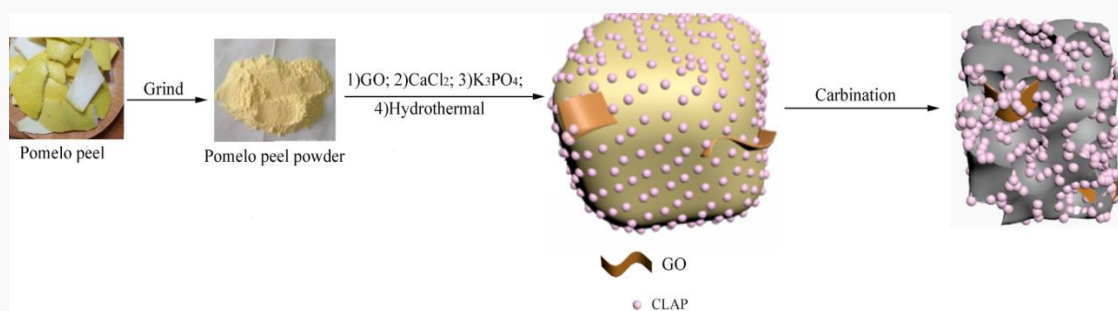
2. Experimental details

2.1. Materials

The pomelo peel was obtained from Changde district of Hunan province. Graphene oxide was supplied by Deyang Carbonene technology Co. Ltd. Calcium chloride dihydrate ($\text{CaCl}_2 \cdot 2\text{H}_2\text{O}$, 99%), potassium phosphate tribasic (K_3PO_4 , 98%) were purchased from Aladdin Co. Ltd.

2.2. Materials synthesis

First, 20.0 g of pomelo peel was placed in a 120 °C oven for 2 h and the obtained solid was milled into powders. Then, 2 g of pomelo powder, 5 mL of graphene oxides solution ($1\text{mg}\cdot\text{mL}^{-1}$), 3.92 g of $\text{CaCl}_2 \cdot 2\text{H}_2\text{O}$ were mixed in the 15 mL deionized water and stirred for 2 hours. Following, 15 ml of K_3PO_4 aqueous ($0.36\text{g}\cdot\text{mL}^{-1}$) was added into the mixed solution drop by drop and continuous stirred for 30 min. After that, the mixed solution was transferred into autoclave and kept the constant temperature of 160 °C for 30 min. The grey product obtained was washed with DI water and ethanol, and dried at 80 °C overnight. Finally, it was heated up to 600 °C in a nitrogen atmosphere at a rate of 5 °C/min, and kept this temperature for 30 min, and then cooled to room temperature. The obtained products were named as BC/G-CLAP. For comparison, the sample prepared under the same conditions but without adding $\text{CaCl}_2 \cdot 2\text{H}_2\text{O}$ and K_3PO_4 was marked as BC/G. The sample BC was prepared according to the conditions of BC/G but without adding GO. G was obtained by heating graphene oxides in the nitrogen atmosphere at 600 °C for 30 min. $\text{CaCl}_2 \cdot 2\text{H}_2\text{O}$ and K_3PO_4 aqueous were reacted in the mixed solution and products were labeled as CLAP. Schem. 1 shows the overall synthesis procedure of BC/G-CLAP.



Scheme 1. Schematics of the preparation of biochar/graphene-supported nano-chlorapatite (BC/G-CLAP).

2.3. Material characterization

The microstructures were characterized by scanning electron microscopy (SEM, Hitachi S4800) and transmission electron microscopy (TEM, JEOL JEM-2100F). The phase was recorded by X-ray diffraction (XRD, Bruker D2 PHASER). Functional groups were investigated using Fourier transform infrared (FTIR) spectroscopy (Nicolet Avatar 370DTGS, USA). The Brunauer-Emmett-Teller (BET) specific surface area of the samples was obtained by nitrogen (N_2) adsorption-desorption experiment (Micromeritics ASAP 2020, USA). The pore size distribution was determined from the Barrett-Joyner-Halenda (BJH) method.

2.4. Pb(II) adsorption in batch experiments

The Pb(II) adsorption experiments are performed operating an $\text{Pb}(\text{NO}_3)_2$ ($100 \text{ mg}\cdot\text{L}^{-1}$) solution at pH 7.0. 10 mg of adsorbents was put into the flask containing 20 mL Pb(II) solution and shaken 200 rpm for 20 h. The samples were taken at scheduled time intervals (from 2 h to 20 h) and then filtered into 10 mL centrifuge tube by $0.45 \mu\text{m}$ filter membrane for further measurements. The equilibrium adsorption amount (q_e , $\text{mg}\cdot\text{g}^{-1}$) was determined by $q_e = (\text{C}_0 - \text{C}_e) \times V/m$, where C_0 and C_e ($\text{mg}\cdot\text{L}^{-1}$) represent the initial and equilibrium concentrations of Pb(II) in the solution, respectively; V (L) is the volume of Pb(II) solution; and m (g) is the mass of the added adsorbent. The residual Pb(II) concentrations were analyzed using inductively coupled plasma-atomic emission spectrometry (ICP-ES, OPTIMA8000, PerkinElmer, USA) for Pb(II).

3. Results and discussion

As shown in Fig. 1, the XRD pattern of CLAP was similar to BC/G-CLAP and the two samples exhibited several diffraction peaks at 28.4, 32.1, 40.5, 46.7 corresponding to (020), (112), (013) and (113) planes of CLAP (JPCDS 27-0074)^[14]. In addition, the diffraction peaks of BC/G-CLAP were sharper than CLAP, indicating a smaller grain size and the well dispersed CLAP in the BC/G-nCLAP composites. Furthermore, an obvious and broad diffraction peak at nearly 25° accounted for the graphitic reflection of (002) plane^[15].

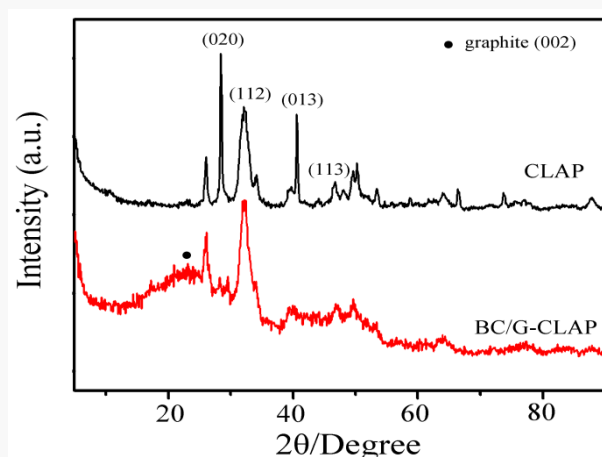


Fig. 1. XRD of the samples.

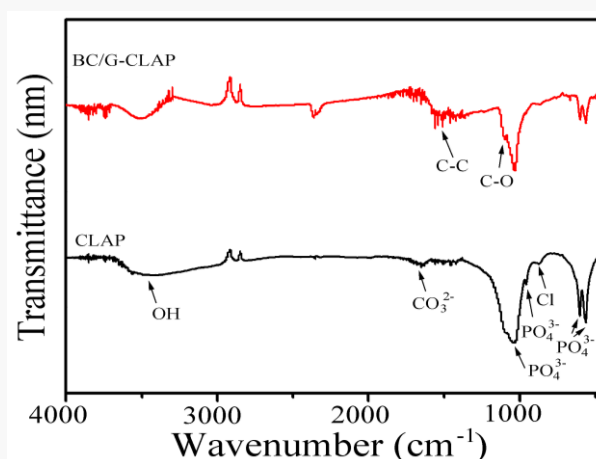


Fig. 2. FTIR spectra of the samples.

The FTIR spectra of CIAP and BC/G-CLAP were depicted in Fig. 2. As for CLAP, the following characteristic peaks were evident: OH stretching vibration due to H₂O at 3415 cm⁻¹, CO₃²⁻ vibrations at 1650 cm⁻¹, and PO₄³⁻ vibrations at 1030, 959, 603, and 564 cm⁻¹. Compared with CIAP, the new peaks of BC/G-CLAP were observed at 1650 cm⁻¹ (the in-plane vibrations of sp² hybridized C-C bonding) and at 1090 cm⁻¹ (alkoxy C-O stretching)^[16]. This result indicated that the biochar/graphene-CLAP had been successfully prepared.

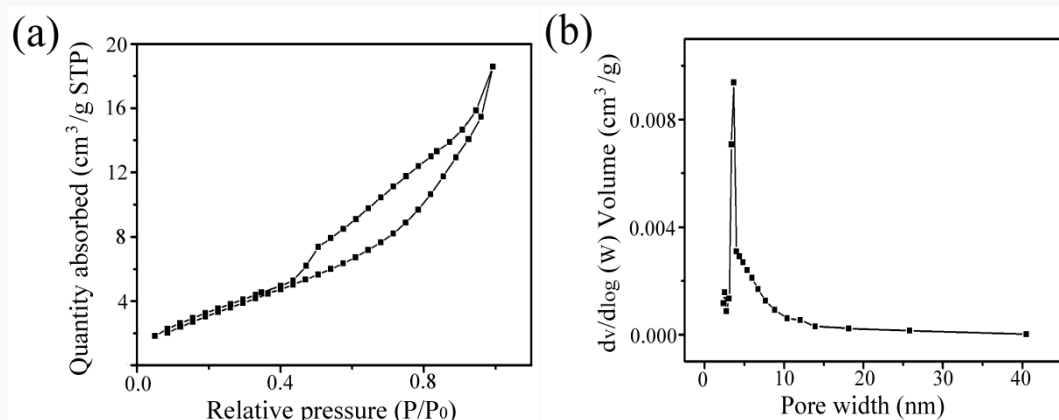


Fig. 3(a) N₂ adsorption-desorption isotherm curves, (b) pore distribution of the BC/G-CLAP samples.

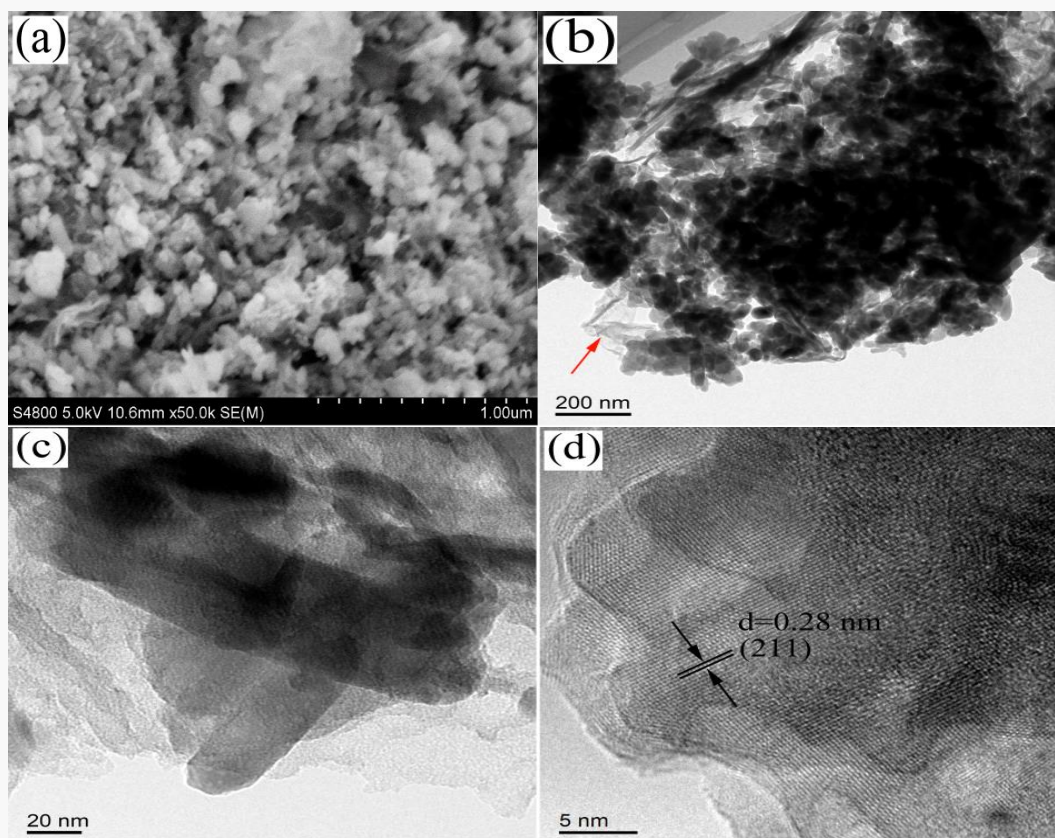


Fig. 4. (a)SEM, (b)(c) TEM, (d)HRTEM of BC/G-CLAP.

The specific surface areas and pore structure characteristics of BC/G-CLAP were analyzed by nitrogen adsorption-desorption. As shown in Fig. 3a, the N₂ adsorption-desorption isotherms of synthesized BC/G-CLAP exhibited type-IV profile with H-1 type hysteresis loop, which was representative of mesoporous structure in the composites. The BET surface area was reached to 13.56 cm².g⁻¹. The BJH pore size distribution (Fig. 3b) showed that BC/G-CLAP had an average pore diameter of about 4 nm and the total pore volume was 0.344 cm³.g⁻¹, indicating that BC/G-CLAP had a uniform pore size in the composites. Hence, with the large BET surface area and abundant mesopores, BC/G-CLAP may achieve the advantage of unique properties for remediation purposes^[17].

The morphology of the BC/G-CLAP was examined by SEM, TEM, and HRTEM. As shown in Fig. 4a, the BC/G-CLAP had a clear porous structure with abundant nanoparticles distributed on their surface. TEM (Fig. 4b) further confirmed that nano particles with the average diameter about 100 nm were distributed on the surface of BC/G. In addition, a wrinkle sheet (as arrow indicates) at the edge of biochar indicated that graphene are distributed on biochar surfaces bearing cavities. The enlarged TEM image (Fig. 4c) clearly showed that biochar, CLAP and graphene were coexisted in the composites. High resolution TEM (HRTEM) image (Fig. 4d) showed the lattice fringes with the interlayer spacing of 0.28 nm, which could be assigned to the (211) plane of CLAP^[18].

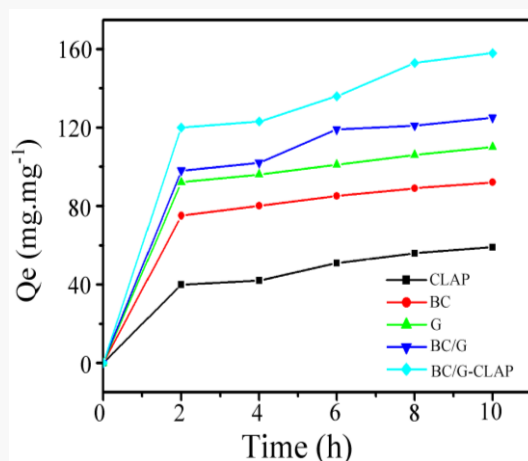
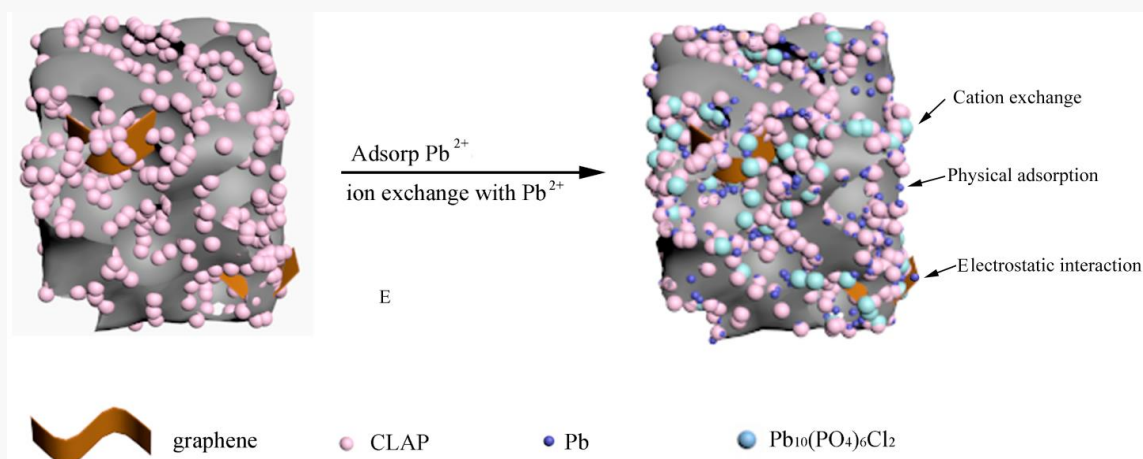


Fig. 5. Adsorption capacity of the samples.

As shown in Fig. 5, the adsorption capacity of Pb(II) on CLAP, BC, G, and BC/G was 59 mg.g⁻¹, 92 mg.g⁻¹, 110 mg.g⁻¹, 125 mg.g⁻¹, respectively. While BC/G-CLAP could reach to 158 mg.g⁻¹, which is nearly 2.68, 1.72, 1.44, 1.26 times higher than CLAP, BC, G, BC/G. Thus, BC/G-CLAP had the maximum adsorption capacity for Pb(II) in aqueous solution. It was supposed that biochar with porous structure, graphene with functional group and the well dispersibility of CLAP were beneficial to the removing of metal ions.



Scheme 2. Possible removal mechanisms of Pb(II) by BC/G-CLAP.

The schematic diagram for the possible removal mechanisms of BC/G-CLAP had been presented in Schem. 2. As BC/G-CLAP provided mesopores structure, abundant functional group, and had abundant CLAP nanoparticles on their surface. Thus these unique properties showed the following ways for the removing of Pb(II) ions^[19,20]. (1) Biochar with porous structure could absorb a small amount of Pb(II) ions; (2) graphene with oxygen-containing groups adsorbed Pb(II) through electrostatic interaction; (3) CLAP could highly form cation exchange with the Pb(II) to form stable $\text{Pb}_{10}(\text{PO}_4)_6\text{Cl}_2$.

4. Conclusions

Biochar/graphene-supported chlorapatite was successfully synthesized for Pb(II) removing in polluted water in this study. The synthesized products were characterized by SEM, TEM, FTIR, and BET. Remediation experiment demonstrated that BC/G-CLAP could remove the Pb(II) ions effectively. The remediation mechanism was discussed and physical adsorption, electrostatic interaction, and cation exchange were involved. This study provides a scientific reference in the production of carbonaceous nano-chlorapatites materials and a great potential for the application for efficient removal of heavy metal.

Acknowledgments

This work was supported by the Natural Science Foundation of China(NSFC, No. 51802096), the Construct Program of the Key Discipline in Hunan Province and Project of the Natural Science Foundation of Hunan Province (2017JJ2191), Key project of Hunan Provincial Education Department (18A361) and the general project of Hunan Provincial Education Department (20C1258).

References

- [1] Z. Zhang, T. Wang, H. Zhang, et al., *Sci Total Environ.* 757, 143910 (2021); <https://doi.org/10.1016/j.scitotenv.2020.143910>
- [2] P. Goyal, C.S. Tiwary, S.K. Misra. *Environ. Manage.* 277, 111469 (2021); <https://doi.org/10.1016/j.jenvman.2020.111469>
- [3] J.M. Wang, J. Zhao, X.Z. Qin, et al., *Mater. Today*, 45, 7290 (2021);

<https://doi.org/10.1016/j.mattod.2020.11.022>

[4] L. Chen, V.K. Ponnusamy, S.L. Hsieh, et al., *J Alloys Compd.* 892, 162015 (2022);

<https://doi.org/10.1016/j.jallcom.2021.162015>

[5] N.J. Jiang, R. Liu, Y.J. Du, et al., *Sci. Total Environ.* 672, 722 (2019);

<https://doi.org/10.1016/j.scitotenv.2019.03.294>

[6] G. Skibsted, L.M. Ottosen, M. Elektorowicz, et al., *J Hazard. Mater.* 358, 459 (2018);

<https://doi.org/10.1016/j.jhazmat.2018.05.033>

[7] B.L. Zhang, W. Qiu, P.P. Wang, et al., *Chem. Eng. J.* 385, 123507 (2020);

<https://doi.org/10.1016/j.cej.2019.123507>

[8] J. Wan, G. Zeng, D. Huang, et al., *J Hazard. Mater.* 343, 332 (2018);

<https://doi.org/10.1016/j.jhazmat.2017.09.053>

[9] R. Deng, D. Huang, W. Xue, et al., *Chem. Eng. J.* 397, 125396 (2020);

<https://doi.org/10.1016/j.cej.2020.125396>

[10] J. Liu, J. Jiang, Y. Meng, et al., *J Hazard. Mater.* 388, 122026 (2020);

<https://doi.org/10.1016/j.jhazmat.2020.122026>

[11] M. Alam, B. Bishop, N. Chen, et al., *Sci. Rep.* 10, 19007 (2020);

<https://doi.org/10.1038/s41598-020-75924-7>

[12] D. Huang, R. Deng, J. Wan, et al., *J Hazard. Mater.* 348, 109 (2018);

<https://doi.org/10.1016/j.jhazmat.2018.01.024>

[13] W. Yu, L. Sisi, Y.H. Yan, et al., *RSC Adv.* 10, 15328 (2020);

<https://doi.org/10.1039/D0RA01068E>

[14] X. Han, Y. Zhang, C.M. Zheng, et al., *Chemosphere*, 264, 128421 (2021);

<https://doi.org/10.1016/j.chemosphere.2020.128421>

[15] B. Zeng, Z. G. Li, W.J. Zeng. *Dig. J Nanomater. Bios.* 16, 627 (2021).

[16] B. Zeng, W.J. Zeng. *Dig. J Nanomater. Bios.* 14, 627 (2019).

[17] B. Keochaiyom, J. Wan, G.M. Zeng, et al., *J Colloid Inter. Sci.* 505, 824 (2017);

<https://doi.org/10.1016/j.jcis.2017.06.056>

[18] P.R. Choudhury, S. Majumdar, S. Sarkar, et al., *Chem. Engin. J.* 355, 510 (2019);

<https://doi.org/10.1016/j.cej.2018.07.155>

[19] X. Han, Y. Zhang, C.M. Zheng, et al., *Chemosphere*, 264, 128421 (2021);

<https://doi.org/10.1016/j.chemosphere.2020.128421>

[20] R.L. Gao, Q.L. Fu, H.Q. Hu, et al., *J Hazard. Mater.* 371, 191 (2019).

<https://doi.org/10.1016/j.jhazmat.2019.02.079>